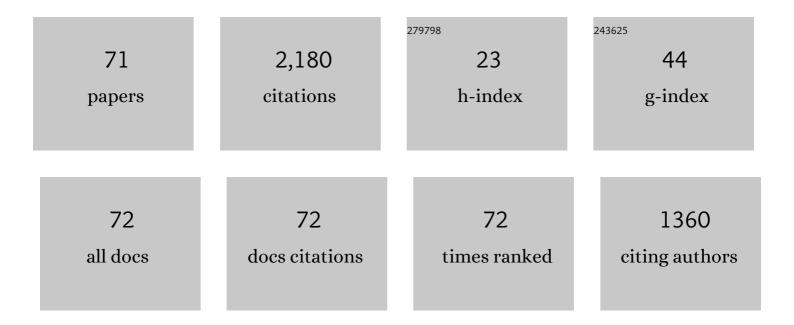
Stoichko Antonov

List of Publications by Year in descending order

Source: https://exaly.com/author-pdf/9576113/publications.pdf Version: 2024-02-01



#	Article	IF	CITATIONS
1	Thermal cycling creep properties of a directionally solidified superalloy DZ125. Journal of Materials Science and Technology, 2022, 104, 269-284.	10.7	14
2	Hot deformation behavior and flow stress modeling of a novel CoNi-based wrought superalloy. Journal of Alloys and Compounds, 2022, 894, 162489.	5.5	19
3	Grain boundary segregation and its implications regarding the formation of the grain boundary α phase in the metastable l²-Titanium Ti–5Al–5Mo–5V–3Cr alloy. Scripta Materialia, 2022, 207, 114320.	5.2	28
4	Effect of pre-strain on hydrogen embrittlement of high manganese steel. Materials Science & Engineering A: Structural Materials: Properties, Microstructure and Processing, 2022, 834, 142596.	5.6	6
5	Atom probe analysis of electrode materials for Li-ion batteries: challenges and ways forward. Journal of Materials Chemistry A, 2022, 10, 4926-4935.	10.3	20
6	Mapping the creep life of nickel-based SX superalloys in a large compositional space by a two-model linkage machine learning method. Computational Materials Science, 2022, 205, 111229.	3.0	10
7	In-situ synchrotron-based high energy X-ray diffraction study of the deformation mechanism of δ-hydrides in a commercially pure titanium. Scripta Materialia, 2022, 213, 114608.	5.2	5
8	The role of β pockets resulting from Fe impurities in hydride formation in titanium. Scripta Materialia, 2022, 213, 114640.	5.2	1
9	Origin of morphological variation of grain boundary precipitates in titanium alloys. Scripta Materialia, 2022, 214, 114651.	5.2	6
10	Unveiling the Re effect on long-term coarsening behaviors of γ′ precipitates in Ni-based single crystal superalloys. Acta Materialia, 2022, 233, 117979.	7.9	32
11	Improved Creep and Tensile Properties of a Corrosion Resistant Ni-Based Superalloy Using High Temperature Aging and Nb/Ta Additions. Metallurgical and Materials Transactions A: Physical Metallurgy and Materials Science, 2022, 53, 2600-2613.	2.2	5
12	Effect of solute atoms (C, Al and Si) on hydrogen embrittlement resistance of high-Mn TWIP steels. Corrosion Science, 2022, 203, 110376.	6.6	7
13	Hydriding of titanium: Recent trends and perspectives in advanced characterization and multiscale modeling. Current Opinion in Solid State and Materials Science, 2022, 26, 101020.	11.5	15
14	Nucleation and growth of α phase in a metastable β-Titanium Ti-5Al-5Mo-5V-3Cr alloy: Influence from the nano-scale, ordered-orthorhombic O″ phase and α compositional evolution. Scripta Materialia, 2021, 194, 113672.	5.2	15
15	Enhanced creep performance in a polycrystalline superalloy driven by atomic-scale phase transformation along planar faults. Acta Materialia, 2021, 202, 232-242.	7.9	29
16	Unveiling True 3D Nanoscale Microstructural Evolution in Chalcogenide Nanocomposites: A Roadmap for Advanced Infrared Functionality. Advanced Optical Materials, 2021, 9, 2002092.	7.3	5
17	Modeling solid solution strengthening in high entropy alloys using machine learning. Acta Materialia, 2021, 212, 116917.	7.9	87
18	Partitioning of Solutes at Crystal Defects in Borides After Creep and Annealing in a Polycrystalline Superalloy. Jom, 2021, 73, 2293-2302.	1.9	3

STOICHKO ΑΝΤΟΝΟ

#	Article	IF	CITATIONS
19	Segregation-assisted phase transformation and anti-phase boundary formation during creep of a γ′-strengthened Co-based superalloy at high temperatures. Acta Materialia, 2021, 215, 117099.	7.9	19
20	Effect of alloying elements on the coarsening rate of Î ³ Ê ¹ precipitates in multi-component CoNi-based superalloys with high Cr content. Scripta Materialia, 2021, 202, 114004.	5.2	38
21	On the role of boron, carbon and zirconium on hot cracking and creep resistance of an additively manufactured polycrystalline superalloy. Materialia, 2021, 19, 101193.	2.7	27
22	High-throughput exploration of alloying effects on the microstructural stability and properties of multi-component CoNi-base superalloys. Journal of Alloys and Compounds, 2021, 881, 160618.	5.5	12
23	Twinning behavior and hydrogen embrittlement of a pre-strained twinning-induced plasticity (TWIP) steel. Corrosion Science, 2021, 192, 109791.	6.6	11
24	Shuffle-induced modulated structure and heating-induced ordering in the metastable β-titanium alloy, Ti-5Al-5Mo-5V-3Cr. Scripta Materialia, 2020, 176, 7-11.	5.2	29
25	Solidification rate driven microstructural stability and its effect on the creep property of a polycrystalline nickel-based superalloy K465. Materials Science & Engineering A: Structural Materials: Properties, Microstructure and Processing, 2020, 770, 138530.	5.6	13
26	The role of nano-scaled structural non-uniformities on deformation twinning and stress-induced transformation in a cold rolled multifunctional β-titanium alloy. Scripta Materialia, 2020, 177, 181-185.	5.2	45
27	Sub/micro-structural evolution of a Co–Al–W–Ta–Ti single crystal superalloy during creep at 900°C and 420ÂMPa. Materials Science & Engineering A: Structural Materials: Properties, Microstructure and Processing, 2020, 772, 138791.	5.6	16
28	Evaluation of service conditions of high pressure turbine blades made of DS Ni-base superalloy by artificial neural networks. Materials Today Communications, 2020, 22, 100838.	1.9	8
29	Phase prediction in high entropy alloys with a rational selection of materials descriptors and machine learning models. Acta Materialia, 2020, 185, 528-539.	7.9	206
30	Structure and tensile properties of Mx(MnFeCoNi)100-x solid solution strengthened high entropy alloys. Materialia, 2020, 9, 100539.	2.7	10
31	Synthesis of a Very High Specific Surface Area Active Carbon and Its Electrical Double-Layer Capacitor Properties in Organic Electrolytes. ChemEngineering, 2020, 4, 43.	2.4	33
32	Exploration of Novel Ordering Mechanism in Titanium Alloys Using Atom Probe Tomography and Aberration-corrected Scanning Transmission Electron Microscopy. Microscopy and Microanalysis, 2020, 26, 2078-2079.	0.4	1
33	Unveiling True Three-dimensional Microstructural Evolution in Novel Chalcogenide Nanocomposites as a Route to Infrared Gradient Refractive Index Functionality. Microscopy and Microanalysis, 2020, 26, 3078-3080.	0.4	3
34	Atom Probe Tomographic Investigation of the Solute Segregation to Crystal Defects in Î ³ -phase Co-35Ni-20Cr-10Mo Superalloy. Microscopy and Microanalysis, 2020, 26, 3076-3077.	0.4	0
35	Hydrogen embrittlement behavior of 13Cr-5Ni-2Mo supermartensitic stainless steel. Corrosion Science, 2020, 176, 109046.	6.6	21
36	High temperature creep behavior of a cast polycrystalline nickel-based superalloy K465 under thermal cycling conditions. Materialia, 2020, 14, 100913.	2.7	18

STOICHKO ΑΝΤΟΝΟ

#	Article	IF	CITATIONS
37	Investigations of dislocation-type evolution and strain hardening during mechanical twinning in Fe-22Mn-0.6C twinning-induced plasticity steel. Acta Materialia, 2020, 195, 371-382.	7.9	105
38	The effect of solute segregation to deformation twin boundaries on the electrical resistivity of a single-phase superalloy. Scripta Materialia, 2020, 186, 208-212.	5.2	12
39	Plasticity assisted redistribution of solutes leading to topological inversion during creep of superalloys. Scripta Materialia, 2020, 186, 287-292.	5.2	26
40	Atomic structure and elemental segregation behavior of creep defects in a Co-Al-W-based single crystal superalloys under high temperature and low stress. Acta Materialia, 2020, 190, 16-28.	7.9	45
41	Effects of Cr and Al/W ratio on the microstructural stability, oxidation property and γ′ phase nano-hardness of multi-component Co–Ni-base superalloys. Journal of Alloys and Compounds, 2020, 826, 154182.	5.5	31
42	Novel deformation twinning system in a cold rolled high-strength metastable-β Ti-5Al-5V-5Mo-3Cr-0.5Fe alloy. Materialia, 2020, 9, 100614.	2.7	21
43	Surface Integrity and Oxidation of a Powder Metallurgy Ni-Based Superalloy Treated by Laser Shock Peening. Jom, 2020, 72, 1803-1810.	1.9	6
44	Evaluation and Comparison of Damage Accumulation Mechanisms During Non-isothermal Creep of Cast Ni-Based Superalloys. Minerals, Metals and Materials Series, 2020, , 228-239.	0.4	1
45	Machine learning assisted design of γ′-strengthened Co-base superalloys with multi-performance optimization. Npj Computational Materials, 2020, 6, .	8.7	56
46	Deformation of Borides in Nickel-based Superalloys: a Study of Segregation at Dislocations. Microscopy and Microanalysis, 2019, 25, 2538-2539.	0.4	4
47	Atom Probe Tomography Investigation on the Effect of Ni Additions on the Site Occupation and Partitioning Behavior in Co-Based Superalloys. Microscopy and Microanalysis, 2019, 25, 2546-2547.	0.4	3
48	ICME Framework for Damage Assessment and Remaining Creep Life Prediction of In-Service Turbine Blades Manufactured with Ni-Based Superalloys. Integrating Materials and Manufacturing Innovation, 2019, 8, 509-520.	2.6	5
49	Three-Dimensional Microstructural Characterization of Novel Chalcogenide Nanocomposites for Gradient Refractive Index Applications. Microscopy and Microanalysis, 2019, 25, 2500-2501.	0.4	4
50	Phosphorous behavior and its effect on secondary phase formation in high refractory content powder-processed Ni-based superalloys. Materialia, 2019, 7, 100423.	2.7	13
51	Hot deformation behavior and flow stress modeling of a Ni-based superalloy. Materials Characterization, 2019, 157, 109915.	4.4	47
52	Effective design of a Co-Ni-Al-W-Ta-Ti alloy with high γ′ solvus temperature and microstructural stability using combined CALPHAD and experimental approaches. Materials and Design, 2019, 180, 107912.	7.0	39
53	Evaluation of microstructural degradation in a failed gas turbine blade due to overheating. Engineering Failure Analysis, 2019, 103, 308-318.	4.0	37
54	MnO ₂ -Coated Sulfur-Filled Hollow Carbon Nanosphere-Based Cathode Materials for Enhancing Electrochemical Performance of Li-S Cells. Journal of the Electrochemical Society, 2019, 166, A1355-A1362.	2.9	18

STOICHKO ANTONOV

#	Article	IF	CITATIONS
55	Machine learning assisted design of high entropy alloys with desired property. Acta Materialia, 2019, 170, 109-117.	7.9	445
56	Design and thermomechanical properties of a Î ³ Ê ¹ precipitate-strengthened Ni-based superalloy with high entropy Î ³ matrix. Journal of Alloys and Compounds, 2019, 792, 550-560.	5.5	32
57	Phase stability and thermodynamic database validation in a set of non-equiatomic Al-Co-Cr-Fe-Nb-Ni high-entropy alloys. Intermetallics, 2019, 104, 103-112.	3.9	21
58	The effect of phosphorus on the formation of grain boundary laves phase in high-refractory content Ni-based superalloys. Scripta Materialia, 2019, 161, 44-48.	5.2	22
59	A modified Î, projection model for constant load creep curves-II. Application of creep life prediction. Journal of Materials Science and Technology, 2019, 35, 687-694.	10.7	14
60	A modified Î, projection model for constant load creep curves-I. Introduction of the model. Journal of Materials Science and Technology, 2019, 35, 223-230.	10.7	18
61	MC Carbide Characterization in High Refractory Content Powder-Processed Ni-Based Superalloys. Metallurgical and Materials Transactions A: Physical Metallurgy and Materials Science, 2018, 49, 2340-2351.	2.2	13
62	Comparison of Thermodynamic Predictions and Experimental Observations on B Additions in Powder-Processed Ni-Based Superalloys Containing Elevated Concentrations of Nb. Metallurgical and Materials Transactions A: Physical Metallurgy and Materials Science, 2018, 49, 729-739.	2.2	6
63	Design of Novel Precipitate-Strengthened Al-Co-Cr-Fe-Nb-Ni High-Entropy Superalloys. Metallurgical and Materials Transactions A: Physical Metallurgy and Materials Science, 2018, 49, 305-320.	2.2	52
64	Two Steady-State Creep Stages in Co-Al-W-Base Single-Crystal Superalloys at 1273ÂK/137ÂMPa. Metallurgical and Materials Transactions A: Physical Metallurgy and Materials Science, 2018, 49, 4079-4089.	2.2	24
65	Synchrotron In-Situ Aging Study and Correlations to the γ′ Phase Instabilities in a High-Refractory Content γ-γ′ Ni-Base Superalloy. Metallurgical and Materials Transactions A: Physical Metallurgy and Materials Science, 2018, 49, 3885-3895.	2.2	10
66	Ϊƒ and η Phase formation in advanced polycrystalline Ni-base superalloys. Materials Science & Engineering A: Structural Materials: Properties, Microstructure and Processing, 2017, 687, 232-240.	5.6	54
67	The effect of Nb on grain boundary segregation of B in high refractory Ni-based superalloys. Scripta Materialia, 2017, 138, 35-38.	5.2	23
68	Comparative study of high-temperature grain boundary engineering of two powder-processed low stacking-fault energy Ni-base superalloys. Materials at High Temperatures, 2016, 33, 310-317.	1.0	11
69	Comparison of thermodynamic database models and APT data for strength modeling in high Nb content γ–γ′ Ni-base superalloys. Materials and Design, 2015, 86, 649-655.	7.0	43
70	Precipitate phase stability and compositional dependence on alloying additions in γ‑'γ′‑'δ‑'Ε Ni-base superalloys. Journal of Alloys and Compounds, 2015, 626, 76-86.	5.5	83
71	Precipitate Phase Stability in γ-γ′-δ-Ε Ni-Base Superalloys. Jom, 2014, 66, 2478-2485.	1.9	17